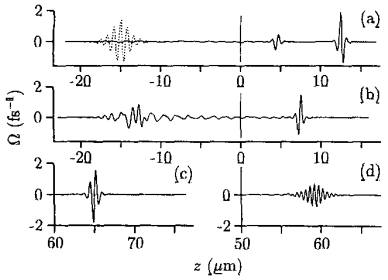

CWF19 Fig. 1. Electric field profiles for different time moments and medium densities (a, b) near the input face at $z = 0$ and (c, d) outside the exit face at $z = 45$ μm: (a) $t = 0.1$ ps, $N = 3 \times 10^{19}$ cm^{-3}; (b) $t = 0.1$ ps, $N = 15 \times 10^{19}$ cm^{-3}; (c) $t = 0.3$ ps, $N = 3 \times 10^{19}$ cm^{-3}; (d) $t = 0.4$ ps, $N = 15 \times 10^{19}$ cm^{-3}.

sponding to the envelope area $A = 4\pi$. For the case of lower density in Fig. 1a the reflection is weak and the penetrating part is strong enough to split into two pulses. In the case of a more dense medium [Fig. 1(b)] a significant part of radiation with low-frequency oscillations on the back front is reflected from the boundary. As seen, in comparison with input (dotted line) the penetrating pulse is significantly shortened up to almost a single cycle.

The propagation of a more intense incident pulse with $E_0 = 5.7 \times 10^9$ V/m and $A = 12.5\pi$ in a more dense medium with $N = 3 \times 10^{20}$ cm^{-3} is presented in Fig. 2. In this case the reflected pulse is rather weak and the penetrating part splits mainly into three pulses with different field strengths and velocities [Fig. 2(a)]. With further propagation these pulses evolve into a higher-frequency oscillating pulse and two separated half-cycle pulses of opposite polarity [Fig. 2(b)]. Both unipolar half-cycle pulses with a duration <1 fs are not attenuated with further long-term propagation and show a clear solitary behavior. As known the existence of self-induced transparency is restricted by the validity of SVEA and RWA, which is violated for the conditions considered here. However, there exists an exact nonoscillating solitary solution[2] of the full Maxwell-Bloch equation describing an unipolar half-cycle pulse. The numerically obtained half-cycle solutions and the analytical soliton solution given in Ref. 2 can be clearly identified with each other. The fastest blue-shifted pulse

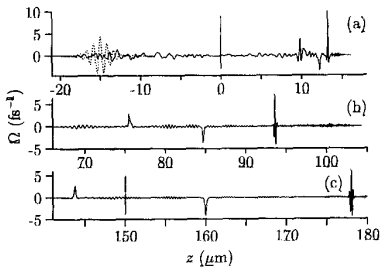

CWF19 Fig. 2. Electric field profiles (a) near the input face at $z = 0$, (b) inside the medium and (c) near output face at $z = 150$ μm; (a) $t = 0.1$ ps; (b) $t = 0.4$ ps; (c) $t = 0.7$ ps.

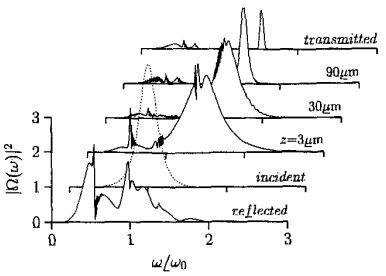

CWF19 Fig. 3. Evolution of the pulse spectrum during propagation inside and outside medium for $N = 15 \times 10^{19}$ cm^{-3}, $A = 4\pi$.

shows also a solitary behavior and represents the two-soliton solution of Maxwell-Bloch equations without SVEA and RWA describing localized pulses with "internal" oscillations.[3]

In Fig. 3 the evolution of the pulse spectrum during propagation through a 150-μm thick layer is presented for the case $E_0 = 1.8 \times 10^9$ V/m and $N = 15 \times 10^{19}$ cm^{-3}. As seen the reflected pulse shows a large red shift with a spectrum maximum position at approximately 0.5 ω_n, where ω_n is the input carrier frequency. On the other hand, the main part of the penetrating pulse spectrum exhibits a blue shift with a maximum at 1.5 ω_n. The physical interpretation of the observed spectral transformation during the propagation is given by intra-pulse third-order difference frequency mixing of the type $2\omega' - \omega'' \rightarrow \omega$. Using a static mode description the analysis of the phase-matching condition shows that for collinear forward propagation only a blue and for backward propagation only a red shift is possible.

**Also at Institute for Nuclear Problems, Belarus State University*

1. M. Nisoli *et al.*, Opt. Lett. **22,** 522 (1997).
2. R.K. Bullough and E. Ahmad, Phys. Rev. Lett. **27,** 330 (1971).
3. J.C. Eilbeck *et al.*, J. Phys. A. **6,** 1337 (1973).

CWF20

Spectral broadening in hollow-core fibers as a function of input chirp

Kyoungsik Kim, Zenghu Chang, Haiwen Wang, Henry C. Kapteyn, Margaret M. Murnane, *Center for Ultrafast Optical Science, University of Michigan, Ann Arbor, Michigan 48109-2099 USA; E-mail: kimkz@umich.edu*

Gas filled hollow core fibers are an ideal nonlinear-optical medium for the spectral broadening of high energy ultrashort pulses, and these fibers have been used to compress 20 fs sub-mJ pulses down to ~5 fs.[1] The spectral broadening of laser pulses is due to the self-phase modulation (SPM) in the gas that fills the fiber. Since SPM induces a positive chirp to the pulse, the initial temporal phase of the input pulse should have an effect on the broadening. We demonstrated experimentally that output spectral width depends strongly on

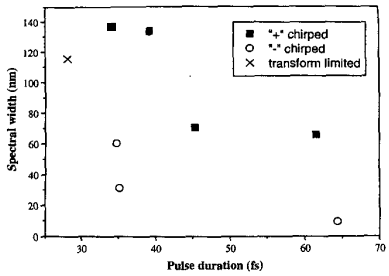

CWF20 Fig. 1. Influence of the input pulse chirp on the spectral width of the output pulse from a hollow-core fiber filled with air. Positively-chirped input pulses result in much broader output spectra than negatively chirped input pulses.

the chirp of the input pulse and can be used to optimize it.

Past work has shown that negatively chirped input pulses in solid core fibers can induce spectral narrowing on an ultrashort pulses.[2] To our knowledge, these effects have not been investigated in detail in the case of the hollow core fiber. Experimentally, we found that largest broadening occurs for slightly positively-chirped input pulses.

We used a 22-cm-long air-filled optical fiber of 450 μm diameter. The laser pulse was 0.5 mJ energy, with a transform-limited pulse duration of 28 fs centered at 800 nm. We varied the chirp of the input pulses by adjusting the separation of the stretcher of the CPA laser. We used frequency resolved optical gating (FROG) to measure the pulse duration and the chirp of the input pulses. The measured spectra of the pulse from the fiber are shown in Fig. 1. It is obvious that the output spectra corresponding to positively chirped pulses is much broader than that with the negatively chirped input pulse. Most interestingly, the broadest spectrum of output beam is when the input pulses are not transform-limited but have a slight positive chirp.

When the input pulse is negatively chirped, it reduces the positive chirp from the SPM, leading to a narrower spectrum. On the other hand, for positively chirped input pulses, the initial chirp enhances the SPM.

1. M. Nisoli *et al.*, Opt. Lett. **22,** 522 (1997).
2. M. Oberthaler *et al.*, Appl. Phys. Lett. **63,** 1017 (1993).

CWF21

Photodiode-based phase-retrieval ultrafast waveform measurements

Tai-Wei Yau, Yuan-Yu Jau,* Chau-Hwang Lee,** and Jyhpyng Wang,† *Institute of Electro-Optical Engineering, National Taiwan University, P.O. Box 23-166, Taipei 106, Taiwan; E-mail: jwang@ltl.iams.sinica.edu.tw*

Frequency-resolved optical gating (FROG) is becoming a standard method for characterizing the amplitude and phase of ultrashort pulses.[1] In FROG, optical waveform is calculated from the power spectrum of the autocor-

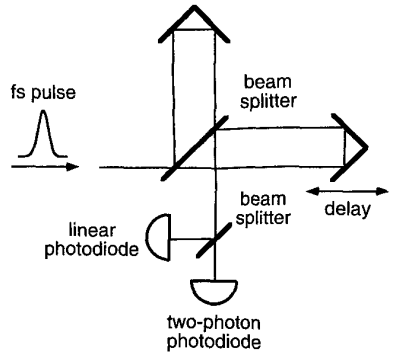

CWF21 Fig. 1. Experimental set-up.

relation signal generated by nonlinear wave mixing. As discussed in Ref. 2, nonlinear wave mixing has the following disadvantages: (1) To measure sub-50-fs pulses, a crystal as thin as several tens of micrometers is required to avoid dispersion-induced pulse broadening and to ensure a sufficiently broad phase-matching bandwidth. (2) Wave mixing in thin nonlinear crystals is intrinsically an inefficient process. This sets a limit on the sensitivity. We developed a phase-retrieval waveform measurement technique by using only photodiodes. Because the nonlinear signal was obtained from two-photon-induced photocurrent,[2] the above disadvantages were eliminated.

The experimental set-up is shown in Fig. 1. When the optical delay line is scanned, the output of the linear silicon photodiode oscillates at a period of $\lambda/2$. The oscillating signal is the field autocorrelation $G_1(\tau)$. In the mean time the output from the GaAsP two-photon photodiode oscillates at a period of $\lambda/4$. The oscillating signal is the second-harmonic field autocorrelation $F_{SH}(\tau)$:

$$F_{SH}(\tau) = \int E^2(t)E^{*2}(t-\tau)dt. \quad (1)$$

The $\lambda/4$ oscillating signal sits on a slowly varying background, which is the intensity autocorrelation $G_2(\tau)$. After Fourier transformation, $G_1(\tau)$ gives $|E(\omega)|$, the power spectrum of $E(t)$; $G_2(\tau)$ gives $|I(\omega)|$, the power spectrum of $I(t)$; and $F_{SH}(\tau)$ gives $|U(\omega)|$, the power spectrum of $E^2(t)$. It has been shown that $|E(\omega)|$, $|I(\omega)|$, and $|U(\omega)|$ together contain enough information to determine the field distribution $E(t)$, up to the time-reversal ambiguity.[3] Our phase-retrieval algorithm starts from the measured $|E(\omega)|$ and an initial guess of the phase $\phi(\omega)$, which generate the trial field $E_i(t)$. From $E_i(t)$ we calculate $I_i(\omega)$ and $U_i(\omega)$. By retaining their phases while replacing the calculated $|I_i(\omega)|$ and $|U_i(\omega)|$ with measured data, we approach the actual $E(t)$ by iteration. Near the end of iteration, when the improvement slows down, we speed up the convergence by using the functional derivative with respect to $\phi(\omega)$ to minimize the difference between the calculated and the measured $G_2(\tau)$ and $F_{SH}(\tau)$.

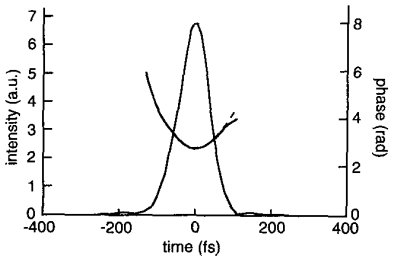

CWF21 Fig. 2. Solid lines: The retrieved intensity and phase profiles of pulses after passing through 2.5-cm BK7 glass. Dashed line: the expected phase profile.

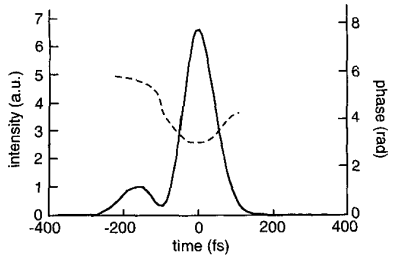

CWF21 Fig. 3. Solid line: The retrieved intensity profile of a double-peak pulse. Dashed line: the retrieved phase profile.

We use pulses synthesized from a transform-limited Kerr-lens mode-locked Ti: sapphire laser to verify the effectiveness of this method. Figure 2 shows the intensity and phase of the pulses after propagating through 2.5-cm BK7 glass. The measured phase curvature and the change of pulse duration agree well with the expected waveform calculated from dispersion data. To show the capability of the method in measuring complex waveforms, we use a double-peak waveform, which is known to be a difficult case for FROG,[4] for the test. The double-peak pulses are synthesized by splitting the pulses at a 1:7 power ratio, delaying the smaller one by 150 fs, passing the larger one through 2.5-cm BK7 glass, then recombining them before the measurement. Figure 3 shows the retrieved double-peak waveform. The errors of the retrieved power ratio and delay are less than 4%.

The sensitivity of this method is great enough for measuring the waveform of nanojoule pulses stretched to hundreds of picoseconds. This makes it a convenient tool for characterizing amplifier seeds and synthesized pulses. The set-up is also simple enough that the whole system can be fabricated as a standard part of femtosecond lasers.

*Department of Physics, National Taiwan University
**Institute of Atomic and Molecular Sciences, Academia Sinica, Taipei, Taiwan
†Also with the Institute of Atomic and Molecular Sciences, Academia Sinica

1. D.J. Kane and R. Trebino, Opt. Lett. **18**, 823 (1993).
2. J.K. Ranka, *et al.*, Opt. Lett. **22**, 1344 (1997).
3. K. Naganuma, *et al.*, IEEE J. Quantum Electron. **25**, 1225 (1989).
4. K.W. DeLong and R. Trebino, J. Opt. Soc. Am. A **11**, 2429 (1994).

CWF22

Rapid amplitude-phase reconstruction of femtosecond pulses from intensity autocorrelation and spectrum

Andrius Baltuška, Audrius Pugžlys, Maxim S. Pshenichnikov, Douwe A. Wiersma, *Ultrafast Laser and Spectroscopy Laboratory, Department of Chemistry, University of Groningen, Nijenborgh 4, 9747 AG Groningen, The Netherlands; E-mail: A.Baltuska@chem.rug.nl*

The retrieval of time-dependent intensity and phase of femtosecond laser pulses is a long-standing problem. To the date, frequency-resolved optical gating (FROG)[1] is probably the most trustworthy pulse measurement method. However, it requires a substantial experimental and numerical involvement. This motivates the quest for other simpler high-fidelity pulse measuring techniques.

In this contribution we present a new method of deciphering the pulse structure from the intensity autocorrelation trace $AC(\tau)$ and the intensity spectrum $S(\omega)$. We show that such a set of data is sufficient to restore the intensity and phase of a femtosecond pulse except for the typical uncertainties concerning the time shift and direction. The main feature of the proposed method is its robustness and swift convergence. Unlike a two-step pulse reconstruction,[2] our algorithm employs the time- and frequency-domain data simultaneously, which in general[3] provides a much faster convergence.

The input data are converted into two arrays each containing N data points (Fig. 1). The iterative algorithm attempts to obtain the best match for the measured autocorrelation trace by varying the spectral phase $\varphi(\omega)$. The rms difference δ (the algorithm error) between the input autocorrelation trace and the one computed for the current guess of $\varphi(\omega)$ is minimized by Davidon-Fletcher-Powell variable metric method.[4] A successful convergence of the iterative algorithm results in the complete amplitude and phase reconstruction of the pulse. The proposed method is incredibly fast because it employs one-dimensional Fourier transforms.

To prevent possible algorithm stagnation, we represent $\varphi(\omega)$ by a cubic spline drawn through m ($m < N$) selected values of the

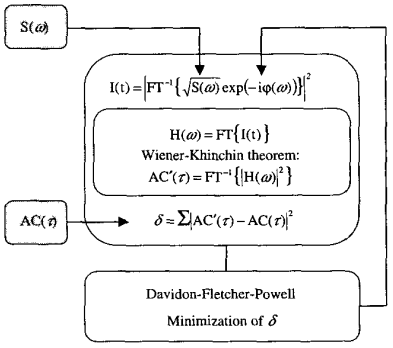

CWF22 Fig. 1. Schematic of the iterative algorithm for pulse characterization from intensity autocorrelation $AC(\tau)$ and spectrum $S(\omega)$.